N. Jb. Miner. Abh.
2008, Vol. 184/3, p. 243–253, Stuttgart, March 2008, published online 2008

V^{3+}-bearing, Mg-rich, strongly disordered olenite from a graphite deposit near Amstall, Lower Austria: A structural, chemical and spectroscopic investigation

Andreas Ertl, George R. Rossman, John M. Hughes, Chi Ma and Franz Brandstätter

With 4 figures and 6 tables

Abstract: An optical absorption spectrum, structural and chemical data of green V- and Cr-bearing tourmaline from the graphite deposit at Weinberg Mountain, west of the village of Amstall, Lower Austria, were obtained. To address the role of V and Cr in the spectrum of tourmaline, examination of additional samples of V- and Cr-containing tourmalines was conducted. This study confirmed that V and Cr produce similar spectra in tourmalines. However, the wavelengths of the 600 nm region band (E\\c), and the 440 nm region band (E⊥c) varied in relation to the proportion of Cr in the sample. Likewise, the intensity of the 680 nm region spin-forbidden bands varies in proportion to the absolute amount of Cr in the sample. Molar absorption coefficients for both V and Cr in tourmaline were determined for the 600 nm region. For the E⊥c band, ε(V) = 12.3 ± 0.7; ε(Cr) = 39.7 ± 1.4; and for the E\\c band, ε(V) = 11.9 ± 2.0; ε(Cr) =15.9 ± 2.8. In each case the Cr bands are more intense than the corresponding V band.

These features can be used to confirm that the spectroscopic features of the Amstall tourmaline come dominantly from V. The optimized formula, calculated using structural and chemical data for the core of a 4 mm wide crystal, is $^{X}(Na_{0.69}Ca_{0.16}K_{0.01}\square_{0.14})$ $^{Y}(Al_{1.46}Mg_{1.34}V^{3+}_{0.11}Ti^{4+}_{0.05}Cr^{3+}_{0.02}Fe_{0.02})$ $^{Z}(Al_{4.77}Mg_{1.23})$ $(BO_3)_3$ $^{T}(Si_{5.70}Al_{0.30})$ O_{18} $[(OH)_{3.87}O_{0.13}]$, with a = 15.984(2), c = 7.222(2) Å, R = 0.017. The optimized formula, calculated using structural and chemical data for the rim, is $^{X}(Na_{0.67}Ca_{0.24}K_{0.01}\square_{0.08})$ $^{Y}(Al_{1.57}Mg_{1.24}V^{3+}_{0.11}Ti^{4+}_{0.05}Cr^{3+}_{0.02}Fe_{0.01})$ $^{Z}(Al_{4.84}Mg_{1.16})$ $(BO_3)_3$ $^{T}(Si_{5.90}Al_{0.10})$ O_{18} $[(OH)_{3.35}O_{0.65}]$, with a = 15.9175(5), c = 7.1914(4) Å, R = 0.014. Whereas the V^{3+} and Cr^{3+} contents stay constant, Mg decreases from the core to the rim. This is reflected by decreasing <*Y*-O> (from 2.013 to 2.003 Å) and <*Z*-O> distances (from 1.938 to 1.930 Å). The relative short <*Y*-O> distances and the enlarged <*Z*-O> distances show that Al and Mg are strongly disordered between the *Y* and *Z* sites in this tourmaline. We assume that the strong Mg-Al disorder between the *Y* and the *Z* sites in this tourmaline derived from a high-*T* overprint (~750 °C, ~6–9 kbar) during crystallization, which is supported by a relatively high amount of $^{[4]}$Al and low vacancies at the *X* site.

Key words: V-bearing, Mg-rich olenite, optical spectrum, crystal structure, chemical analyses, disorder.

Introduction

Green, vanadium-bearing, magnesium-rich tourmaline from the mountain Weinberg, approximately 500 m west of the village of Amstall, Lower Austria, occurs in small quartz-feldspar dikes in graphite schist. Ertl (1995), in his summary of the mineral paragenesis from this large graphite deposit, gave unit-cell parameters and the results of semi-quantitative chemical analyses, but in the preliminary report those author did not note that these tourmaline samples are vanadium-bearing. From the same locality, Hughes et al. (Submitted) described V-rich $2M_1$ muscovite with the highest reported V^{3+} content noted in that phase to date (V_2O_3 = 11.35 wt%).

Hawthorne & Henry (1999) gave the general chemical formula of the tourmaline-group minerals as $X\ Y_3\ Z_6\ [T_6O_{18}]\ (BO_3)_3\ V_3\ W$ [*V* site = O3 site, *W* site = O1 site]. The *Z* site in tourmaline can be occupied by Al, Mg, Fe^{3+}, V^{3+} and Cr^{3+}. The substitution of Al for Mg at the *Z* site was described by Grice & Ercit (1993), Hawthorne et al. (1993), MacDonald & Hawthorne (1995), Taylor et al. (1995), Bloodaxe et al. (1999), Ertl et al. (2003a), Bosi & Lucchesi (2004), and Bosi et al. (2004).

Vanadium-containing tourmalines, including gem varieties, have previously been described from Kenya and Tanzania (Bassett 1953, Zwaan 1974). Their spectroscopy and other properties were studied in detail by Schmetzer (1978, 1982), Schmetzer & Bank (1979), and Platonov & Tarashchan (1973).

DOI: 10.1127/0077-7757/2008/0100
0077-7757/08/0100 $ 2.75

The structure of V-rich dravite was first described by Foit & Rosenberg (1979). Structures and chemistry of V-bearing to V-rich (and Cr-rich) tourmalines from Siberia, Russia, were recently described by Bosi & Lucchesi (2004) and Bosi et al. (2004).

Regional geology and description of mineralogy of the quartz-feldspar dikes

The graphite deposit near Amstall occurs within the Bunte Series (tectonic Drosendorf unit) of the Austrian part of the Moldanubian zone (see sampling area in Fig. 1). Petrakakis et al. (1999) suggested that the Bunte Series is an old segment of crust containing a composite Proterozoic gneissic basement overlain by a late Proterozoic and/to Silurian, shelf and slope-derived, pelite- and carbonate-rich, volcano-sedimentary succession. Graphite from this deposit, which is silica-rich, originated due to metamorphosis of sapropel and shows a higher degree of crystallinity (Holzer 1963, 1964, Holzer & Zirkl 1962, Zirkl 1961). Graphite is also a characteristic mineral in the gneisses, quarzites, and marbles of the Bunte Serie (Petrakakis et al. 1999). *PT* estimates of the metamorphic conditions derived from typical Grt+Sil+Kfs+Bt-gneisses and some Grt+Opx-amphibolites were given

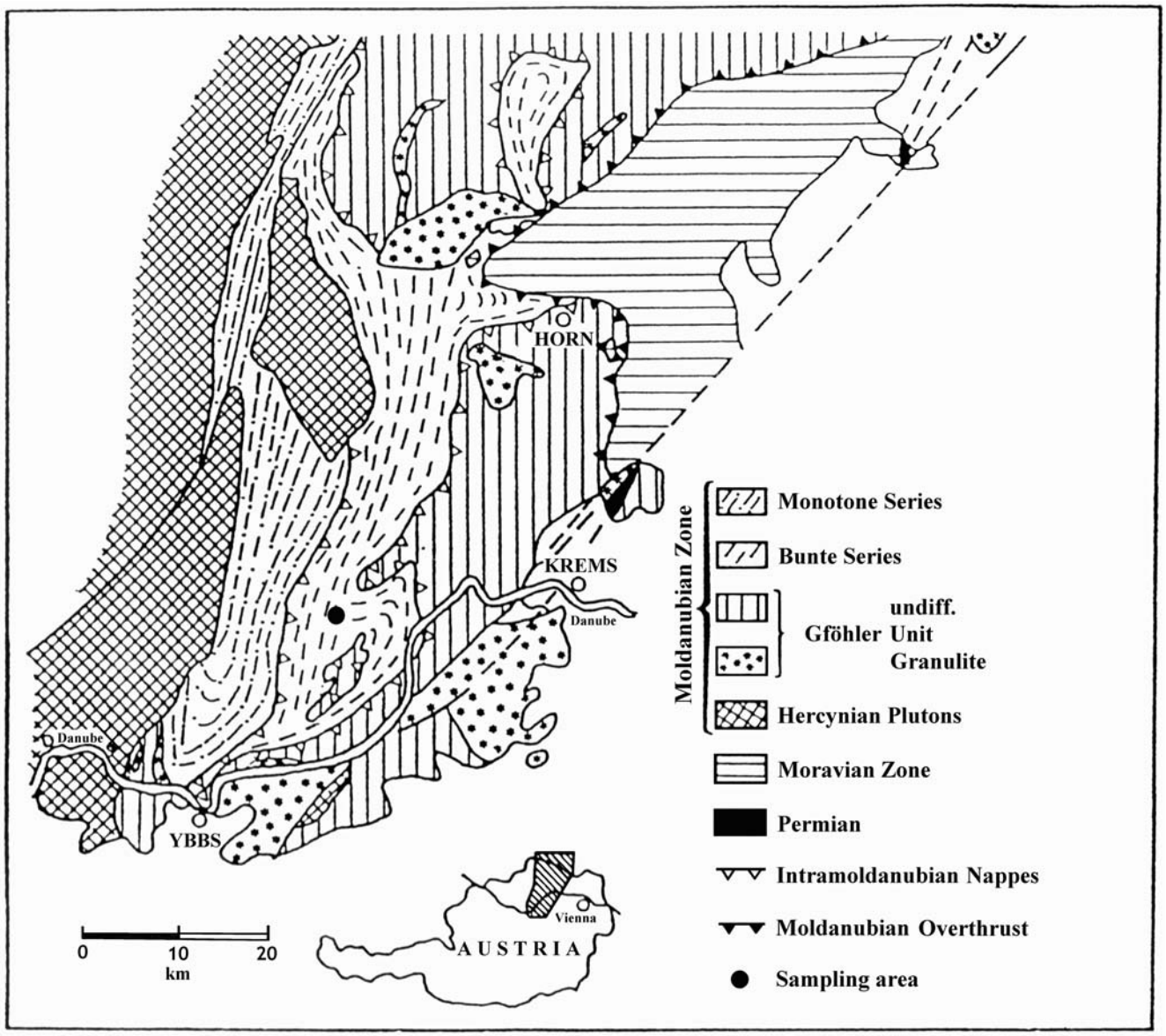

Fig. 1. Simplified geological map of the Austrian part of the Moldanubian zone after Scharbert & Fuchs (1981) and Petrakakis & Jawecki (1995).

from PETRAKAKIS (1997) and PETRAKAKIS et al. (1999) as 7–11 kbar/700–800 °C (a_{H2O}<<1; see also PETRAKAKIS & JAWECKI 1995). This Variscan MP/HT event (around 340 Ma) was accompanied by strong decompression-induced anatexis of fertile lithologies (PETRAKAKIS et al. 1999). An overview of the geochronological data is given by KLÖTZLI et al. (1999). Although the graphite deposit is also assumed to be of Proterozoic origin, the quartz-feldspar dikes (containing tourmaline) within the graphite schist could be related to a decompression-induced anatexis during a younger (Variscan?) metamorphic event.

The quartz-feldspar dikes contain albite, oligoclase, orthoclase, quartz, muscovite (V-bearing to V-rich), sillimanite, pyrite, jarosite, natrojarosite, rutile, titanite, apatite, vivianite, xenotime-(Y), monazite-(Ce?), allanite-(Ce), amstallite, siderite, calcite, and laumontite, (summarized by Ertl 1995). Tourmaline crystals (usually up to 2 mm in length, rarely up to 2 cm) occur sometimes in pyrite-rich quartz-feldspar dikes.

Experimental details

Sample selection

A green short prismatic tourmaline crystal (VDR0, ~1 mm in width; ~2 mm in length) from the described graphite deposit near Amstall, Lower Austria, was used for the spectroscopic investigations. Pieces from the rim (VDR1) and from the core (VDR2) were separated from a second green short prismatic tourmaline crystal (~4 mm in width, ~7 mm in length). These euhedral crystals are intergrown with feldspar and graphite and show the forms {101}, {120} and {010}. The two pieces (VDR1, VDR2) were first used for structure refinements and subsequently for chemical analysis. Samples of a variety of other green to yellow-green tourmalines from East Africa and Myanmar containing both V and Cr were selected for optical absorption studies (Table 1). They were generally clear, transparent fragments of crystals. The sample of GRR 2128 was obtained by slicing off the outermost 2 mm clear rim of an otherwise turbid crystal.

Table 1. V- and Cr-bearing tourmaline samples from different localities.

Sample	Locality and description
VDR0	Green, prismatic crystal from a graphite quarry, Amstall, west of Mühldorf, Waldviertel, Lower Austria, Austria
GRR 768	Fragments of a dark green fluor-rich uvite from an unspecified locality in Kenya
GRR 1719	Fragments of a dark green dravite crystal from an unspecified locality in Tanzania
GRR 2128	A 1.5 cm cluster of green, euhedral crystals of V-containing uvite from the Mogok region, Myanmar
GRR 2467	Fragments of a yellow-green uvite crystal from an unspecified locality in Tanzania.
GRR 2396	Crystal sections of a dark, yellowish-green fluor-rich uvite from an unspecified locality in Kenya

Optical spectra

Optical absorption spectra were obtained on a microspectrometer consisting of a 1024 element silicon diode array connected to a highly modified SpectraTech NicPlan® infrared microscope using a pair of conventional 10× objectives as objective and condenser. Polarized spectra were obtained with a calcite polarizer at a spectroscopic resolution of about 1 nm using a sampling area of 100 ×100 µm in the clearest central portion of the crystal. Doubly-polished slabs of each crystal were prepared that contained the *c*-axis in the plane of the slab. The thicknesses of the samples used for measurements are: VDR0, 0.629 mm; GRR768, 1.204 mm; GRR 1719, 2.076 mm; GRR 2128, 1.111 mm; GRR 2467, 2.258 mm. The spectrum of a synthetic, Cr-doped olenite originally presented by TARAN et al. (1993), retaken on a 0.278 mm thick sample, was provided by M.N. Taran.

Near-infrared spectra

The near-infrared spectrum of VDR0 was obtained on a Thermo-Nicolet Magna 860 FTIR using a CaF_2 beamsplitter and a LN_2-cooled MCT-A detector. The spectrum was obtained over the 9000–2500 cm^{-1} range in a 1 mm diameter region of the crystal dominated by the core portion of the crystal. Total integrated absorbance was determined in the region of the first overtone of the OH stretch using the formula $Abs_{total} = 2\times \int Abs_{(\perp c)} + \int Abs_{(\parallel c)}$. The water content was determined from an ongoing, currently unpublished study of the correlation between the integrated near-IR intensities and the total "water" contents of the tourmaline group.

Crystal structure

The same crystals (VDR1, VDR2; ~50 µm in diameter) that were used for chemical analyses were mounted on a Bruker Apex CCD diffractometer equipped with graphite-monochromated Mo $K\alpha$ radiation. Refined cell-parameters and other crystal data are listed in Table 2. Redundant

Table 2. Crystal data and results of structure refinement for V-bearing, Mg-rich olenite from Amstall, Lower Austria.

Space group: *R*3*m*	
Unit cell parameters (Å):	
VDR1: a = 15.9175(5), c = 7.1914(4)	VDR2: a = 15.984(2), c = 7.222(2)
Frame width, scan time, number of frames, detector distance: 0.20^0, 15 s, 4500, 5 cm	
Measured reflections, full sphere:	
VDR1: 11,593	VDR2: 11,527
Unique reflections; refined parameters:	
VDR1: 1,133; 94	VDR2: 1,145; 94
$R1$, $I > 4\sigma_I$:	
VDR1: 0.0136	VDR2: 0.0172
Difference peaks (+,–):	
VDR1: 0.34, 0.22	VDR2: 0.42, 0.36
Goodness-of-Fit:	
VDR1: 0.439	VDR2: 1.190

data were collected for an approximate sphere of reciprocal space, and were integrated and corrected for Lorentz and polarization factors using the Bruker program SAINT-PLUS (Bruker AXS Inc. 2001).

The structure was refined using tourmaline starting models and the Bruker SHELXTL v. 6.10 package of programs, with neutral-atom scattering factors and terms for anomalous dispersion. Refinement was performed with anisotropic thermal parameters for all non-hydrogen atoms. In Table 3, we list the atom parameters, and in Table 4, we present selected interatomic distances.

Chemical analysis

The two single crystals used for the structure refinement were analyzed with a wavelength-dispersive ARL SEMQ electron microprobe (EMP) at the Natural History Museum, Vienna, Austria (Table 5). Accelerating voltage was

Table 3. Atomic positions equivalent isotropic U for atoms in V-bearing, Mg-rich olenite from Amstall, Lower Austria.

VDR1 (rim):

ATOM	*X*	*Y*	*Z*	U_{EQ}	*OCC.*
Na	0	0	3/4	0.0179(4)	$Na_{1.030(7)}$
Si	0.80836(2)	0.81025(2)	0.9768(2)	0.00674(9)	$Si_{1.00}$
B	0.89035(6)	0.7807(1)	0.5230(3)	0.0082(3)	$B_{1.00}$
AlY	0.87652(3)	0.93826(2)	0.3416(2)	0.0110(2)	$Al_{1.014(4)}$
AlZ	0.70236(2)	0.73867(2)	0.3660(2)	0.0074(1)	$Al_{0.991(3)}$
O1	0	0	0.2073(3)	0.0115(3)	$O_{1.00}$
O2	0.93955(4)	0.87910(8)	0.4908(2)	0.0130(2)	$O_{1.00}$
O3	0.7385(1)	0.86925(5)	0.4661(2)	0.0153(2)	$O_{1.00}$
O4	0.90662(4)	0.81325(9)	0.9044(2)	0.0122(2)	$O_{1.00}$
O5	0.81610(9)	0.90805(4)	0.8835(2)	0.0125(2)	$O_{1.00}$
O6	0.80560(5)	0.81561(6)	0.1998(2)	0.0105(2)	$O_{1.00}$
O7	0.71466(5)	0.71503(5)	0.8986(2)	0.0104(2)	$O_{1.00}$
O8	0.79089(5)	0.73001(6)	0.5371(2)	0.0116(2)	$O_{1.00}$
H3	0.742(2)	0.871(1)	0.584(4)	0.039(8)	$H_{1.00}$

VDR2 (core):

ATOM	*X*	*Y*	*Z*	U_{EQ}	*OCC.*
Na	0	0	1/4	0.02086(11)	$Na_{0.996(1)}$
Si	0.19165(2)	0.18976(2)	0.0213(2)	0.0074(1)	$Si_{1.00}$
B	0.10974(7)	0.2195(1)	0.4756(3)	0.0087(3)	$B_{3.00}$
AlY	0.12378(4)	0.06189(2)	–0.3442(2)	0.0120(2)	$Al_{1.020(1)}$
AlZ	0.29770(2)	0.26139(3)	–0.3678(2)	0.0082(1)	$Al_{0.996(3)}$
O1	0	0	–0.2083(3)	0.0120(4)	$O_{1.00}$
O2	0.06066(5)	0.12132(9)	0.5077(3)	0.0136(3)	$O_{1.00}$
O3	0.2617(1)	0.13087(6)	–0.4681(3)	0.0160(3)	$O_{1.00}$
O4	0.09339(5)	0.1868(1)	0.0933(3)	0.0129(2)	$O_{1.00}$
O5	0.1841(1)	0.09203(5)	0.1142(3)	0.0131(2)	$O_{1.00}$
O6	0.19465(6)	0.18456(6)	–0.2015(2)	0.0109 (2)	$O_{1.00}$
O7	0.28527(6)	0.28488(6)	0.0996(2)	0.0110(2)	$O_{1.00}$
O8	0.20915(6)	0.27003(7)	0.4611(2)	0.0122(2)	$O_{1.00}$
H3	0.260(2)	0.130(1)	0.417(5)	0.038(9)	$H_{1.00}$

Table 4. Selected interatomic distances (Å) in V-bearing, Mg-rich olenite from Amstall, Lower Austria.

	VDR1 (rim)	**VDR2** (core)
X-		
O2 (x3)	2.501(1)	2.507(2)
O5 (x3)	2.711(1)	2.730(2)
O4 (x3)	2.804(1)	2.823(2)
Mean	**2.672**	**2.687**
Y-		
O1	1.957(1)	1.974(1)
O6 (x2)	1.9802(9)	1.992(1)
O2 (x2)	1.9973(8)	2.0057(9)
O3	2.103(1)	2.109(2)
Mean	**2.003**	**2.013**
Z-		
O8	1.8967(8)	1.9037(9)
O6	1.9015(9)	1.908(1)
O7	1.9054(8)	1.9135(9)
O8'	1.9271(8)	1.935(1)
O7'	1.9542(8)	1.9628(9)
O3	1.9933(6)	2.0021(7)
Mean	**1.930**	**1.938**
T-		
O7	1.6054(7)	1.6109(9)
O6	1.6076(9)	1.6127(11)
O4	1.6265(4)	1.6323(5)
O5	1.6422(5)	1.6480(6)
Mean	**1.6204**	**1.6260**
B-		
O2	1.375(1)	1.378(2)
O8 (x2)	1.376(2)	1.380(1)
Mean	**1.376**	**1.379**

15 kV, beam current 15 nA, and spot size 2 µm. Natural silicates and oxides were used as standards. Under the described conditions, analytical errors on all analyses are ± 3 % relative for major elements and 5 % relative for minor elements.

The amount of B_2O_3 was calculated as B = 3.00 *apfu* by assuming that there is no $^{[4]}$B in this tourmaline sample. This assumption is supported by the structure refinements and also by the <*T*-O> distances of ≥1.620 Å (Table 3). The ideal <*T*-O> bond length (*T* site fully occupied with Si) has been determined to be ~1.620 Å by various structural studies (MacDonald & Hawthorne 1995, Bloodaxe et al. 1999, Ertl et al. 2001).

The amount of H_2O was calculated based on (OH+F) = 3.5 *pfu* following the results of Novák et al. (2004) who found that the normalization of electron-microprobe data of (Fe,Mg)-rich, (Ca,Li,F)-poor tourmalines from granitic pegmatites is generally satisfied based on $(OH,F)_{3.5}O_{0.5}$. The OH content in the optimized formulae was calculated for charge-balanced formulae (see also Bosi & Lucchesi 2004). The near-infrared spectrum confirms the validity of this calculation.

Analyses of the other tourmalines were conducted with a JEOL 8200 electron microprobe at the California Institute of Technology. To optimize the analysis of the low concentrations of V and Cr, beam current of 40 nA was employed at 15 kV accelerating voltage and 10 µm defocused spot size. Standards for the analysis were albite (Na*K*α), anorthite (Ca*K*α, Al*K*α, Si*K*α), forsterite (Mg*K*α), fayalite (Fe*K*α), Cr_2O_3 (Cr*K*α), V_2O_3 (V*K*α), phlogopite (F*K*α), Mn-olivine (Mn*K*α), TiO_2 (Ti*K*α) and ZnO (Zn*K*α). Spectral interferences of V *K*α by Ti and Cr Kα by V were corrected. Analyses were processed with the CITZAF correction procedure (Armstrong 1995).

Optimization of site occupancies

Using quadratic programming methods, Wright et al. (2000) offer a method of optimizing the site occupancies of cation sites in minerals with multiply occupied cation sites; the optimized formula essentially minimizes the differences between the formula obtained from the results of the chemical analysis and that obtained by SREF. Using that method with the structure refinement and chemical data obtained in this study, the structural formulae of these tourmaline samples are:

VDR1 (rim): $^{X}(Na_{0.67}Ca_{0.24}K_{0.01}\square_{0.08})\ ^{Y}(Al_{1.57}Mg_{1.24}V^{3+}_{0.11}Ti^{4+}_{0.05}Cr^{3+}_{0.02}Fe_{0.01})\ ^{Z}(Al_{4.84}Mg_{1.16})\ (BO_3)_3\ ^{T}(Si_{5.90}Al_{0.10})\ O_{18}\ [(OH)_{3.35}O_{0.65}]$

VDR2 (core): $^{X}(Na_{0.69}Ca_{0.16}K_{0.01}\square_{0.14})\ ^{Y}(Al_{1.46}Mg_{1.34}V^{3+}_{0.11}Ti^{4+}_{0.05}Cr^{3+}_{0.02}Fe_{0.02})\ ^{Z}(Al_{4.77}Mg_{1.23})\ (BO_3)_3\ ^{T}(Si_{5.70}Al_{0.30})\ O_{18}\ [(OH)_{3.87}O_{0.13}]$

The valence state of Fe could not be obtained by Mössbauer spectroscopy due to the very low FeO content (Table 1).

Results and discussion

Cause of color. The optical spectrum of VDR0 (Fig. 2) contains absorption bands with maxima at about 438 and 608 nm (E⊥c) and 438 and 608 nm (E\\c). These positions are consistent with those observed previously in vanadium-containing tourmalines (Schmetzer 1982). The spectrum and the dominance of vanadium in the chemical analysis suggest that vanadium is the primary cause of color and is present in the 3+ oxidation state in an approximately octahedral site.

A potential complication comes from the fact that chromium is also present in the Amstall tourmaline in

Table 5. Composition of V-bearing, Mg-rich olenite from Amstall, Lower Austria (wt.%).

	VDR1 (rim)[1]	VDR1 (rim)[2]	VDR2 (core)[1]	VDR2 (core)[2]
SiO_2 wt.%	36.47	36.66	35.40	35.52
TiO_2	0.44	0.41	0.41	0.41
B_2O_3	10.82[3]	10.80	10.76[3]	10.83
Al_2O_3	34.36	34.33	34.76	34.52
Cr_2O_3	0.17	0.16	0.13	0.16
V_2O_3	0.84	0.85	0.85	0.85
FeO	0.11	0.07	0.14	0.15
MnO	0.03	–	0.03	–
MgO	10.24	10.01	10.66	10.74
CaO	1.30	1.39	0.74	0.93
Na_2O	1.94	2.15	2.11	2.22
K_2O	0.05	0.05	0.06	0.05
H_2O	3.27[4]	3.12	3.24[4]	3.62
Sum	100.04	100.00	99.29	100.00
Si *apfu*	5.85	5.90	5.73	5.70
[4]Al	0.15	0.10	0.27	0.30
Sum *T* site	6.00	6.00	6.00	6.00
[3]B	3.00	3.00	3.00	3.00
Al	6.35	6.41	6.36	6.23
Cr^{3+}	0.02	0.02	0.02	0.02
V^{3+}	0.11	0.11	0.11	0.11
Fe^{2+}	0.01	0.01	0.02	0.02
Mn	0.00	–	0.00	–
Mg	2.45	2.40	2.57	2.57
Ti	0.05	0.05	0.05	0.05
Sum *Y*, *Z* sites	8.99	9.00	9.13	9.00
Ca	0.22	0.24	0.13	0.16
Na	0.60	0.67	0.66	0.69
K	0.01	0.01	0.01	0.01
Sum *X* site	0.83	0.92	0.80	0.86
Sum cations	18.82	18.92	18.93	18.86
Sum OH	3.50[4]	3.35[5]	3.50[4]	3.87[5]

Note: [1] Average of 3 EMP analyses. [2] Wt. percent calculated from optimal site occupancies and normalized to 100%. A component is not considered significant unless its value exceeds the uncertainty. [3] B_2O_3 calculated as B = 3.00. [4] H_2O was calculated for (OH + F) = 3.5 (Novák et al. 2004). F was below the detection limit. [5] OH in the optimized formulae was calculated for charge-balanced formulae.

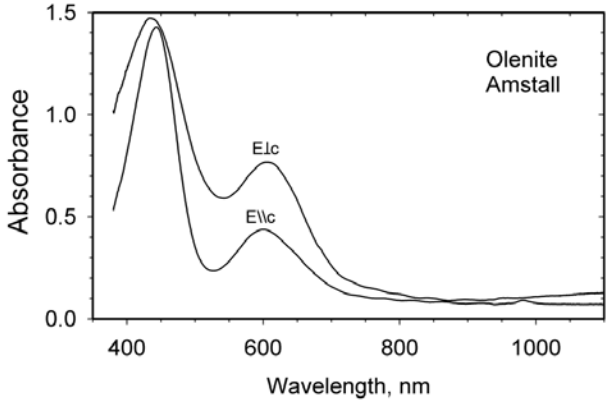

Fig. 2. Optical absorption spectrum of a 0.629 mm thick crystal of the V^{3+}-bearing, Mg-rich olenite from Amstall, Lower Austria, plotted normalized to 1.0 mm thickness.

lesser amounts. In tourmalines, chromium occurs in the 3+ oxidation state and has an optical absorption spectrum that closely resembles V^{3+} in band position. No information is available about the quantitative intensities of absorption of V^{3+} and Cr^{3+} in tourmaline.

A significant difference is the frequent obvious presence of a series of sharp bands in the 680–690 nm region (from spin-forbidden transitions) in Cr^{3+} spectra that are barely visible in V^{3+} spectra. Low intensities in the spin-forbidden region suggest that V^{3+} is the dominate cause of color in the Amstall olenite.

To address the issues regarding the role of V and Cr in the spectrum of tourmaline, examination of additional samples of V- and Cr-containing tourmalines was conducted (Table 1). Samples were chosen in the uvite-drav-

ite-olenite series that contained different concentrations of V and Cr that ranged from V-dominant to Cr-dominant. This study confirmed that V and Cr produce similar spectra in tourmalines (Fig. 3). However, the wavelengths of the 600 nm region band (E\\c), and the 440 nm region band (E⊥c) varied in relation to the proportion of Cr in the sample (Fig. 4a,b). Likewise, the intensity of the 680 nm region spin-forbidden bands varies in proportion to the absolute amount of Cr in the sample. These features are sufficiently diagnostic that they can be used to confirm that the spectroscopic features of the Amstall tourmaline come dominantly from V.

Also relevant is a spectrum of a synthetic tourmaline containing Cr^{3+} that is presented by Taran et al. (1993). Although it bears much similarity to the spectra of V^{3+} in tourmalines, there are some differences that distinguish it from the spectrum of the Amstall tourmaline. A prominent band in the Cr^{3+} spectrum is centered at 596 nm compared to 610 nm in the Amstall tourmaline as well as vanadian tourmalines from Tanzania. The sharp, spin forbidden band of Cr^{3+} occurs at 686 nm in all of the Cr^{3+} and mixed Cr^{3+} /V^{3+} tourmalines. It is significantly more intense in the synthetic Cr-containing tourmaline than it is in the Amstall tourmaline even though the Amstall tourmaline contains twice the amount of V than the synthetic tourmaline contains Cr.

This study also makes it possible to determine the molar absorption coefficient (epsilon values) for both V and Cr in the uvite-dravite-olenite series of tourmalines. Using pairs of spectra, simultaneous linear equations involving Cr and V concentrations and total absorption intensities of the E\\c and E⊥c bands in the 600 nm region were solved that yielded the epsilon values for both elements. Multiple pairs from the overdetermined equations were selected that, gratifyingly, yielded nearly the same answers for both epsilon values. For the E⊥c band, ε(V) = 12.3 ± 0.7; ε(Cr) = 39.7 ± 1.4; and for the E\\c band, the values are not as well constrained, but ε(V) = 11.9 ± 2.0; ε(Cr) =15.9 ± 2.8. In each case the Cr bands are more intense than the corresponding V band.

OH Content. The total integrated absorbance of the near-infrared OH overtones in the 7400 cm^{-1} region excluding the ~7600 cm^{-1} band, is 1270 cm^{-2}. Using this value and the calculated density (3.051) and correlations between OH content in tourmalines (Ertl et al. 2006), we estimate that the Amstall tourmaline (VDR0) has 3.32 wt% H_2O. This value lies between the calculated H_2O content (by charge balance) for the core (3.62 wt%; VDR2, Table 5) and the rim composition (3.12 wt%; VDR1, Table 5) of the larger crystal from this locality.

Compositional and structural trends. Using valid current tourmaline end-member species (Hawthorne & Henry 1999), we can describe the tourmaline samples from Amstall essentially as a solid solution of olenite and dravite components. The core sample (VDR2) consists of 49 mol% olenite and 45 mol% dravite. The rim sample (VDR1) consists of 52 mol% olenite and 41 mol% dravite. Whereas the olenite component decreases from the core to the rim, the dravite component increases.

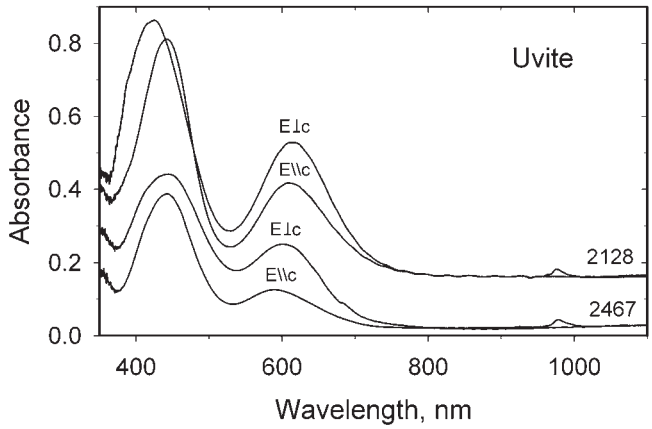

Fig. 3. Comparison of the spectra of Cr-dominant uvite (GRR 2467), and V-dominant uvite (GRR 2128), showing that the 440 nm band (E⊥c) occurs at shorter wavelength than the corresponding Cr band. Also, weak, spin-forbidden bands near 680 nm are apparent in the spectrum of the Cr-dominant uvite. All spectra plotted normalized to 1.0 mm thickness. The spectra of GRR 2128 are offset vertically for clarity.

The CaO content increases from the core to the rim (from 0.74 to 1.30 wt%; Table 1), whereas the Na_2O content does not change significantly. Also the <*X*-O> distance decreases from the core to the rim (from 2.687 to 2.672 Å). An increasing Ca content from the Fe-rich core to the Fe-poor rim was also observed in B-rich olenite (Hughes et al. 2004). Contrary to this investigation, the Fe content in our samples is constantly very low, whereas the Mg content is decreasing from the core to the rim.

Based on optical spectroscopic data, Schmetzer (1982) concluded that "in the tourmaline lattice, [there is] a preference for the smaller Al-site [*Z* site] (rather than the greater Mg-site [*Y* site]) by V^{3+}". However, the optimized formulae show that V^{3+} only occupies the *Y* sites in our tourmalines. Significant V^{3+} contents at the *Z* site were only described from a few tourmalines in the past (up to 0.22–0.38 *apfu*; Foit & Rosenberg 1979, Bosi & Lucchesi 2004, Bosi et al. 2004), whereas usually the major or the whole V^{3+} contents were assigned to the *Y* site (Foit & Rosenberg 1979, McDonald & Hawthorne 1995, Bosi & Lucchesi 2004, Bosi et al. 2004). In all these papers the <*Y*-O> distance was higher (2.020–2.048 Å) than in our samples (2.013 to 2.003 Å; Table 4), ex-

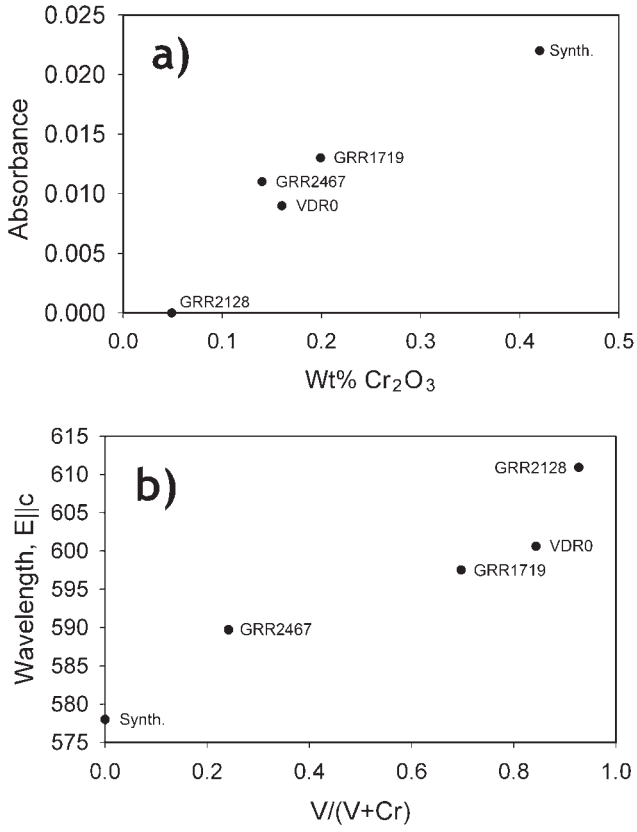

Fig. 4. Dependence of spectral features on the Cr and V content of tourmalines;
a) Absorbance normalized to 1.0 mm thickness of the spin-forbidden band (~680 nm); b) Wavelength position of the 600 nm region band (E\\c) in relation to the proportion of Cr in the tourmaline samples used for the correlations: VDR0, Synthetic, GRR 1719, GRR 2128, GRR 2467.

cept in the $^{Y}Cr^{3+}$-rich tourmalines from Bosi et al. (2004) (1.999–2.002 Å). While the small <*Y*-O> distance in our samples can be explained by relatively high Al contents, the tourmalines from Bosi et al. (2004) have no or very small amounts of Al at the *Y* site (up to 0.097 *apfu*) but are enriched in Cr^{3+} (1.740 to 2.298 *apfu* at the *Y* site). The V^{3+} content does not change significantly from the core to the rim in our Mg-rich olenite from Amstall.

The Si value of the core sample (VDR2; Table 1) with ~5.7 *apfu* is relatively low, but no tetrahedral B was found by crystal structure determination. During refinement no significant change of the scattering value could be observed by releasing the occupancy of the *T* site. In combination with the relatively high <*T*-O> distance of ~1.626 Å we conclude that, in addition to Si, only Al can occupy the *T* site in this Mg-rich tourmaline (cf. MacDonald & Hawthorne 1995). The value of ~0.3 *apfu* $^{[4]}$Al is in good agreement with the observed <*T*-O> distance (Foit & Rosenberg 1979, Ertl et al. 2001, Prowatke et al. 2003). Henry & Dutrow (1996) described 0.25 $^{[4]}$Al *apfu* from tourmalines which have been crystallized above 750 °C. Such tourmalines from high grade metapelites have relatively low vacancies (0.05±0.05) at the *X* site when they crystallized above 750 °C (Henry & Dutrow 1996). Hence, we conclude that these V-bearing tourmalines started crystallizing at temperatures ~750 °C. This is in agreement with the intensive high-*T* overprint of the rocks of the Moldanubian Bunte Series in the range 700–800 °C and 8–11 kbar (Petrakakis 1997). After an approximately isobar decompression down to ~6 kbar isotherm cooling down to ~500 °C followed (see Fig. 7 and 8 in Petrakakis 1997).

The total Mg content decreases from the core to the rim, and is reflected by decreasing <*Y*-O> (from 2.013 to 2.003 Å) and <*Z*-O> distances (from 1.938 to 1.930 Å). The relatively short <*Y*-O> distances and the enlarged <*Z*-O> distances ($^{Z}Al_{6.0}$ produces <*Z*-O> distances in the range 1.902–1.911 Å; Grice & Ercit 1993, Hughes et al. 2000, Ertl et al. 2003b, Prowatke et al. 2003), show that Al and Mg are strongly disordered in these V-bearing tourmaline samples. The tourmaline from Amstall shows the greatest amount of Mg-Al disorder between the *Y* and the *Z* sites of all investigated tourmalines to date. Tourmalines with a large amount of Mg-Al disorder between the *Y* site and the *Z* site were further reported by Ertl et al. (2003a) [up to $Al_{1.58}Mg_{0.91}$ at the *Y* site (<*Y*-O> = 2.006 Å) and $Al_{4.90}Mg_{1.10}$ at the *Z* site (<*Z*-O> = 1.926 Å)], by Bosi & Lucchesi (2004) [V-bearing tourmaline 9840f: $Al_{1.25}Mg_{1.22}$ at the *Y* site (<*Y*-O> = 2.011 Å) and $Al_{4.99}Mg_{0.99}$ at the *Z* site (<*Z*-O> = 1.930 Å)], and by Bloodaxe et al. (1999) [sample LCW 2356: $Al_{1.09}Mg_{1.52}$ at the *Y* site (<*Y*-O> = 2.022 Å) and $Al_{4.98}Mg_{1.02}$ at the *Z* site (<*Z*-O> = 1.926 Å)]. Different methods for the approximate estimation of the Mg content at the *Z* site have been published: Bloodaxe et al. (1999) described a negative correlation between Fe^{2+} on the *Y* site and Mg on *Z*. By using figure 3 from Bloodaxe et al. (1999), ~1.14 *apfu* Mg were assigned to the *Z* site for the tourmaline samples from Amstall. Ertl et al. (2003a) gave another method for approximating the Mg content at the *Z* site. Each lattice parameter for the *c-axis* corresponds to a particular Mg content at the *Z* site. The estimated ^{Z}Mg contents for the tourmaline samples from Amstall are in the range ~1.0–1.3 *apfu* Mg. By using figure 5 (variation in *c* cell constant as a function of <*Z*-O>) of Bosi & Lucchesi (2004), the estimated <*Z*-O> distances for tourmaline sample VDR1 gives ~1.927 Å (measured distance: 1.930 Å; Table 4), and for sample VDR2 it gives ~1.937 Å (measured distance: 1.938 Å; Table 4). By using the measured <*Z*-O> distances and by applying figure 3 (relationship between <*Z*-O> and *Z*-site population) of Bosi &

Table 6. Electron microprobe analyses (wt.%) of other V- and Cr-bearing tourmalines used in this study.

	GRR2128	GRR2396	GRR1719	GRR768	GRR2467	Synthetic*
Na_2O	1.19	0.98	1.51	1.25	1.13	2.17
CaO	3.29	3.46	1.15	3.26	3.16	0.00
MgO	12.61	13.24	9.68	13.74	11.31	0.03
FeO	0.011	0.064	0.002	0.004	0.033	0.15
Cr_2O_3	0.049	0.098	0.199	0.140	0.140	0.42
V_2O_3	0.614	0.294	0.452	0.244	0.044	n.a.
Al_2O_3	30.02	27.53	32.77	26.69	30.40	51.77
SiO_2	35.59	36.39	36.75	36.52	36.04	31.70
F	1.03	1.589	0.25	1.66	0.13	n.a.
MnO	0.001	0.004	0.008	0.010	0.001	0.02
TiO_2	0.16	0.49	0.28	1.02	0.898	0.00
ZnO	0.02	0.04	0.01	0.02	0.019	n.a.
Sum	84.58	84.18	83.05	84.56	83.27	86.26
V/(V+Cr)	0.92	0.75	0.67	0.64	0.22	0.00

Note: * Data (sample no. 10) from Taran et al. (1993) and personal communication (2007). n.a. = not analyzed. The localities of these samples are described in Table 1. The Mg-Al disorder between the Y and the Z sites can not be estimated in these samples without structural data.

Formula proportions

GRR2128:
$(Ca_{0.584}Na_{0.383}\square_{0.033})\ (Mg_{2.889}V^{3+}_{0.082}Ti^{4+}_{0.020}Cr^{3+}_{0.006}Fe_{0.002}Zn_{0.002})\ (Al_{5.771}Mg_{0.229})\ (BO_3)_3\ [Si_{5.902}Al_{0.098}O_{18}]\ (OH)_3\ [F_{0.54}O_{0.31}(OH)_{0.15}]$

GRR2396
$(Ca_{0.611}Na_{0.313}\square_{0.076})\ (Mg_{2.603}Ti^{4+}_{0.061}V^{3+}_{0.039}Cr^{3+}_{0.013}Fe_{0.009}Mn_{0.001}\square_{0.274})\ (Al_{5.349}Mg_{0.651})\ (BO_3)_3\ [Si_{6.00}O_{18}]\ (OH)_3\ [F_{0.83}O_{0.11}(OH)_{0.06}]$

GRR1719:
$(Na_{0.477}Ca_{0.200}\square_{0.323})\ (Mg_{2.356}Al_{0.305}V^{3+}_{0.059}Ti^{4+}_{0.034}Cr^{3+}_{0.026}Mn_{0.001}Zn_{0.001}\square_{0.218})\ Al_6\ (BO_3)_3\ [Si_{6.00}O_{18}]\ (OH)_3\ [O_{0.58}(OH)_{0.29}F_{0.13}]$

GRR768:
$(Ca_{0.574}Na_{0.398}\square_{0.028})\ (Mg_{2.530}Ti^{4+}_{0.126}V^{3+}_{0.032}Cr^{3+}_{0.018}Zn_{0.002}Mn_{0.001}Fe_{0.001}\square_{0.289})\ (Al_{5.166}Mg_{0.834})\ (BO_3)_3\ [Si_{6.00}O_{18}]\ (OH)_3\ [F_{0.86}O_{0.09}(OH)_{0.05}]$

GRR2467:
$(Ca_{0.563}Na_{0.365}\square_{0.071})\ (Mg_{2.772}Ti^{4+}_{0.108}Cr^{3+}_{0.018}V^{3+}_{0.006}Fe_{0.005}Zn_{0.002}\square_{0.089})\ (Al_{5.966}Mg_{0.034})\ (BO_3)_3\ [Si_{6.00}O_{18}]\ (OH)_3\ [O_{0.62}(OH)_{0.31}F_{0.07}]$

Synthetic:
$(Na_{0.662}\square_{0.338})\ (Al_{2.598}Cr^{3+}_{0.052}Fe_{0.020}Mg_{0.007}\square_{0.321}]\ Al_6\ (BO_3)_3\ [Si_{4.991}Al_{1.009}O_{18}]\ (OH)_3\ [O_{0.67}(OH)_{0.33}]$

Lucchesi (2004), we can estimate that the ^{Z}Mg contents for the Amstall tourmaline are in the range ~0.90–1.25 *apfu*. All these methods for approximating the Mg content at the *Z* site give results that are close. We assume that the strong Mg-Al disorder between the *Y* and the *Z* sites in the Amstall tourmaline derived from the relatively high temperature (~750 °C) during crystallization.

Ertl et al. (2002) showed that the bond-angle distortion (σ_{oct}^2) of the ZO_6 octahedron in a tourmaline is largely a function of the <*Y*-O> distance of that tourmaline, although the occupant of the O3 site (*V* site) also affects that distortion. The covariance, *r*, of <*Y*-O> and the σ_{oct}^2 of the ZO_6 octahedron is –0.991 for all investigated tourmalines that are occupied by 3 (OH) groups, including the samples from Hughes et al. (2004). The tourmaline samples from Amstall both fall on the *V* site = 3 (OH) line in figure 3 from Ertl et al. (2002), defining covariance of the relationship between the bond-angle distortion (σ_{oct}^2) of the ZO_6 octahedron and the <*Y*-O> distance. It is only possible to do a semi-quantitative estimation of the OH content of the O3 site by using this relationship. Hence, we assume that the *V* site in VDR1 and VDR2 is filled by ~3.0 (OH). The optimized formula for the core sample (VDR2) gives the *W*-site occupation with $[(OH)_{0.87}O_{0.13}]$, whereas the *W* site for the rim sample (VDR1) is occupied by $[O_{0.65}(OH)_{0.35}]$. F was below the detection limit. The refinement of VDR2 in fact shows a difference peak of +0.42 $e^-/Å^3$ in a distance of 0.57 Å from O1, which can be assigned to H1. No such peak that can be associated with H1 was found in the refinement of VDR1. Hence, we believe that the optimized values of OH for the *W* sites, which do not result from a direct water determination, are approximately correct, which is supported by the water determination of sample VDR0 by using the total integrated absorbance of the near-infrared OH overtones. Sample VDR2 needs more OH for a charge balanced formula than

VDR1, because of the higher deficiency in Si^{4+}, the higher total amount of Mg^{2+} (which is exchanged by Al^{3+}), and the lower amount of Ca^{2+}. Marschall et al. (2004) described a strongly disordered dravite (with a small amount of $^{[4]}B$) where the *W* site is almost completely occupied by OH groups.

The core sample of this V-bearing tourmaline shows that Mg-rich, Fe- and Mn-poor tourmaline with a relatively high Al content at the *Y* site (reflected by a low <*Y*-O> distance; VDR2: 2.013 Å) can have a relatively high lattice parameter *a* (~16.0 Å) when the *Z* site is occupied by a relatively high content of Mg (~1.2 *apfu*), when the <*X*-O> distance (VDR2: 2.687 Å) is relatively large, and when the <*T*-O> distance (VDR2: 1.626 Å) is significantly enlarged.

Acknowledgements

We thank Erwin Löffler, Emmersdorf an der Donau, Lower Austria, for helping with the collection of the tourmaline samples. Julius Petsch (Idar Oberstein, Germany), Herb Obodda (Short Hills, New Jersey, U.S.A.), and William F. Larson (Fallbrook, California, U.S.A.) provided samples used in this study, and Michail Taran (Kiev, Ukraine) provided additional data about his study of synthetic tourmaline. We sincerely thank Pavel Uher (Bratislava, Slovakia) and Yves Fuchs (Marne La Vallee, France) for their careful reviews of the manuscript. This work was supported in part by NSF grants EAR-0125767 and EAR-0337816 to GRR, and EAR-0003201 and EAR-9804768 to JMH.

References

Armstrong, J. T. (1995): CITZAF: a package of correction programs for the quantitative electron microbeam X-ray analysis of thick polished materials, thin films, and particles. – Microbeam Analysis **4**: 177–200.

Bassett, H. (1953): A vanadiferous variety of tourmaline from Tanganyika. – Rec. Geol. Surv. Tanganyika **3**: 93–96.

Bloodaxe, E. S., Hughes, J. M., Dyar, M. D., Grew, E. S. & Guidotti, C. V. (1999): Linking structure and chemistry in the schorl-dravite series. – Amer. Mineral. **84**: 922–928.

Bosi, F. & Lucchesi, S. (2004): Crystal chemistry of the schorl-dravite series. – Eur. J. Mineral. **16**: 335–344.

Bosi, F., Lucchesi, S. & Reznitskii, L. (2004): Crystal chemistry of the dravite–chromdravite series. – Eur. J. Mineral. **16**: 345–352.

Ertl, A. (1995): Elbait, Olenit, Dravit-Buergerit-Mischkristalle, Dravit, Uvit und ein neuer Al-Turmalin (?) von österreichischen Fundstellen. – Mitt. Österr. Miner. Ges. **140**: 55–72.

Ertl, A., Hughes, J. M. & Marler, B. (2001): Empirical formulae for the calculation of <*T*-O> and *X*-O2 bond lengths in tourmaline and relations to tetrahedrally-coordinated boron. – N. Jb. Miner. Mh. **12**: 548–557.

Ertl, A., Hughes, J. M., Pertlik, F., Foit, F. F. Jr., Wright, S. E., Brandstätter, F. & Marler, B. (2002): Polyhedron distortions in tourmaline. – Can. Mineral. **40**: 153–162.

Ertl, A., Hughes, J. M., Brandstätter, F., Dyar, M. D. & Prasad, P. S. R. (2003a): Disordered Mg-bearing olenite from a granitic pegmatite from Goslarn, Austria: A chemical, structural, and infrared spectroscopic study. – Can. Mineral. **41**: 1363–1370.

Ertl, A., Hughes, J. M., Prowatke, S., Rossman, G. R., London, D. & Fritz, E. A. (2003b): Mn-rich tourmaline from Austria: structure, chemistry, optical spectra, and relations to synthetic solid solutions. – Amer. Mineral. **88**: 1369–1376.

Ertl, A., Rossman, G. R., Hughes, J. M., Wang, Y., O'Leary, J., Dyar, M. D., Prowatke, S. & Ludwig, T. (2006): Elbaite from the Himalaya Mine, Mesa Grande, California. – Gems & Gemol. **42**: 96.

Foit, F. F. & Rosenberg, P. E. (1979): The structure of vanadium-bearing tourmaline and its implications regarding tourmaline solid solutions. – Amer. Mineral. **64**: 788–798.

Grice, J. D. & Ercit, T. S. (1993): Ordering of Fe and Mg in the tourmaline crystal structure: The correct formula. – N. Jb. Mineral. Abh. **165**: 245–266.

Hawthorne, F. C., MacDonald, D. J. & Burns, P. C. (1993): Reassignment of cation site-occupancies in tourmaline: Al-Mg disorder in the crystal structure of dravite. – Amer. Mineral. **78**: 265–270.

Hawthorne, F. C. & Henry, D. J. (1999): Classification of the minerals of the tourmaline group. – Eur. J. Mineral. **11**: 201–215.

Henry, D. & Dutrow, B. (1996): Metamorphic tourmaline and its petrologic applications. – Rev. Mineral. **33**: 503–557.

Holzer, H. (1963): Über einige weitere niederösterreichische Graphitlagerstätten. – Verh. Geol. B.-A. **1963**: 79–91.

– (1964): Die Flinzgraphitvorkommen im außeralpinen Grundgebirge Ober- und Niederösterreichs. – Verh. Geol. B.-A. **1964**: 360–371.

Holzer, H. & Zirkl, E. J. (1962): Weitere Mitteilungen über niederösterreichische Graphitlagerstätten. – Verh. Geol. B.-A. **1962**: 316–330.

Hughes, J. M., Ertl, A., Dyar, M. D., Grew, E. S., Shearer, C. K., Yates, M. G. & Guidotti, C. V. (2000): Tetrahedrally coordinated boron in a tourmaline: boron-rich olenite from Stoffhütte, Koralpe, Austria. – Can. Mineral. **38**: 861–868.

Hughes, J. M., Ertl, A., Dyar, M. D., Grew, E. S., Wiedenbeck, M. & Brandstätter, F. (2004): Structural and chemical response to varying $^{[4]}B$ content in zoned Fe-bearing olenite from Koralpe, Austria. – Amer. Mineral. **89**: 447–454.

Hughes, J. M., Ertl, A., Bernhardt, H.-J., Rakovan, J. & Rossman, G. R. (subm.): Vanadium-rich muscovite from Austria: crystal structure, chemical analysis, and spectroscopic investigations. – Can. Mineral.

Klötzli, U. S., Frank, W., Scharbert, S. & Thöni, M. (1999): The evolution of the SE Bohemian Massif based on geochronological data: a review. – Jb. Geol. B.-A. **141/4**: 377–394.

Marschall, H. R., Ertl, A., Hughes, J. M. & McCammon, C. (2004): Metamorphic Na- and OH-rich disordered dravite with tetrahedral boron, associated with omphacite, from Syros, Greece: chemistry and structure. – Eur. J. Mineral. **16**: 817–823.

MacDonald, D. J. & Hawthorne, F. C. (1995): The crystal chemistry of Si ⇔ Al substitution in tourmaline. – Can. Mineral. **33**: 849–858.

Novák, M., Povondra, P. & Selway, J. B. (2004): Schorl-*oxy-schorl* to dravite-*oxy-dravite* tourmaline from granitic pegmatites; examples from the Moldanubicum, Czech Republic. – Eur. J. Mineral. **16**: 323–333.

Petrakakis, K. (1997): Evolution of Moldanubian rocks in Austris: review and synthesis. – J. Metam. Geol. **15**: 203–222.

Petrakakis, K. & Jawecki, C. (1995): High-grade metamorphism and retrogression of Moldanubian granulites, Austria. – Eur. J. Mineral. **7**: 1183–1203.

Petrakakis, K., Klötzli, U. & Richter, W. (1999): Excursion to the Austrian part of Moldanubia. – Beih. z. Eur. J. Mineral. **11**: 61–90.

Platonov, A. N. & Tarashchan, A. N. (1973): Spectroscopy of vanadium in natural minerals. III. Absorption spectra of V^{4+} and V^{3+} complexes. – Konst. Svoistva Miner. **7**: 75–81 (in Russian).

Prowatke, S., Ertl, A. & Hughes, J. M. (2003): Tetrahedrally-coordinated Al in Mn-rich, Li- and Fe-bearing olenite from Eibenstein an der Thaya, Lower Austria: A chemical and structural investigation. – N. Jb. Miner. Mh. **9**: 385–395.

Scharbert, H. G. & Fuchs, G. (1981) Metamorphe Serien im Moldanubikum Niederösterreichs. – Fortschr. Mineral. **59**: 129–152.

Schmetzer, K. (1978): V(III) als Farbträger bei natürlichen Silikaten und Oxiden. Ein Beitrag zur Kristallchemie des Vanadiums. – Diss., Univ. of Heidelberg, Germany.

– (1982): Absorption spectroscopy and color of vanadium(3+)-bearing natural oxides and silicates – a contribution to the crystal chemistry of vanadium. – N. Jb. Mineral. Abh. **144**: 73–106.

Schmetzer, K. & Bank, H. (1979): East African tourmalines and their nomenclature. – J. Gemmology **16**: 310–320.

Taran, M. N., Lebedev, A. S. & Platonov, A. N. (1993): Optical absorption spectroscopy of synthetic tourmalines. – Phys. Chem. Minerals **20**: 209–220.

Taylor, M. C., Cooper, M. A. & Hawthorne, F. C. (1995): Local charge-compensation in hydroxyl-deficient uvite. – Can. Mineral. **33**: 1215–1221.

Wright, S. E., Foley, J. A. & Hughes, J. M. (2000): Optimization of site-occupancies in minerals using quadratic programming. – Amer. Mineral. **85**: 524–531.

Zirkl, E. J. (1961): Vorläufiger Bericht über die mineralogischen Untersuchungen einiger Graphitvorkommen aus dem niederösterreichischen Waldviertel. – Verh. Geol. B.-A. **1961**: 99–101.

Zwaan, P. C. (1974): Garnet, corundum and other gem minerals from Umba, Tanzania. – Scripta Geol. **20**: 1–41.

Received: June 20, 2007; accepted: September 14, 2007.
Responsible editor: A. Beran

Authors' addresses:

Andreas Ertl, Institut für Mineralogie und Kristallographie, Geozentrum, Universität Wien, Althanstrasse 14, 1090 Vienna, Austria. E-mail: andreas.ertl@a1.net

George R. Rossman, Division of Geological and Planetary Sciences, California Institute of Technology, Pasadena, California 91125-2500, U.S.A.

John M. Hughes, Office of the Provost, University of Vermont, 348B Waterman Building, Burlington, Vermont 05405, U.S.A.

Chi Ma, Division of Geological and Planetary Sciences, California Institute of Technology, Pasadena, California 91125-2500, U.S.A.

Franz Brandstätter, Mineralogisch-Petrographische Abteilung, Naturhistorisches Museum, Burgring 7, 1010 Vienna, Austria.